JOURNAL OF SPACECRAFT AND ROCKETS
Vol. 37, No. 1, January–February 2000

Galileo Prime Mission Navigation

R. J. Haw,* P. G. Antreasian,† T. P. McElrath,‡ and G. D. Lewis§
Jet Propulsion Laboratory, California Institute of Technology, Pasadena, California 91109

A summary of the navigation performance of the Galileo spacecraft for the first 11 Jupiter satellite encounters is described. The achieved performance is compared against predicted accuracies. The average target miss in the satellite's B-plane coordinate frame (compared against postencounter reconstruction) was 0.9σ in $B \cdot R$, 0.6σ in $B \cdot T$, and 1.6σ in encounter time, with a largest single error of 3.4σ in $B \cdot R$. This performance preserved sufficient onboard propellant to enable a follow-on mission of up to four years. Knowledge of the Galilean satellite positions has been improved by an order of magnitude. For the first time the low-order gravity coefficients of Io, Europa, Ganymede, and Callisto have been determined, and improvements to the masses of these satellites and Jupiter have been obtained. The gravity results indicate that the Galilean satellites have differentiated into two or more layers. This and other supporting evidence indicates that a layer of liquid water may exist on Europa beneath an ice lithosphere.

Nomenclature

B1950	= planetary ephemeris reference epoch (year 1950)
$B \cdot R$	= see Appendix
$B \cdot S$	= see Appendix
$B \cdot T$	= see Appendix
CT, **DT**, **OOP**	= right-handed unit triad directed along the radial, downtrack, and out-of-plane directions, respectively
C_{22}	= normalized spherical harmonic gravity field coefficient
d	= day
e	= orbit eccentricity
GM	= product of universal gravitational constant G and mass M (km^3/s^2)
G1+apo	= apojove following Ganymede-1 encounter (analogous numbering for subsequent encounters
h	= hour
J2000	= planetary ephemeris reference epoch (year 2000)
J_2, J_4	= normalized spherical harmonic gravity coefficient (oblateness term)
S_{22}	= normalized spherical harmonic gravity coefficient
ΔV	= change in velocity
θ	= see Appendix

Introduction

THE Galileo spacecraft, the first spacecraft to orbit an outer planet, has completed its primary mission and is still functioning at the time of this writing. Jupiter and the four Galilean moons (Io, Europa, Ganymede, and Callisto) have all been closely observed. This paper will describe the navigation results of Galileo's first dozen orbits around Jupiter and compare these results with a priori goals and error analyses. In support of the navigation activities, we also compute new ephemerides and gravity fields for Jupiter and the Galilean moons. Background material on Galileo's mission is documented in the literature.[1–9]

A subset of this paper was presented as Paper 97-699 at the AAS/AIAA Astrodynamics Specialist Conference, 4–7 August 1997; received 1 February 1999; revision received 12 September 1999; accepted for publication 9 October 1999.

*Member of Engineering Staff, Navigation and Mission Design; Robert.Haw@jpl.nasa.gov.

†Member of Engineering Staff, Navigation and Mission Design; P.G.Antreasian@jpl.nasa.gov.

‡Member of Engineering Staff, Navigation and Mission Design; T.P.McElrath@jpl.nasa.gov.

§Member of Engineering Staff, Navigation and Mission Design; G.Lewis@jpl.nasa.gov.

Navigation Strategies

Spacecraft Trajectory

The Galileo spacecraft had completed 12 orbits around Jupiter by the end of 1997, encountering 11 satellites at altitudes between 200 and 3100 km. Each orbit was characterized by a targeted flyby of either Europa, Ganymede, or Callisto and is designated by a letter and a number indicating the satellite and orbit. For example, G2 indicates that Galileo passed closest to Ganymede in its second orbit.

Galileo's trajectory around Jupiter closely approached each targeted satellite so that the gravitational assist would redirect the spacecraft onward to subsequent satellite encounters along a ballistic (or nearly ballistic) path. The dates of each targeted encounter and the achieved altitudes and latitudes are chronicled in Table 1. Important to the mission for additional science opportunities were the so-called nontargeted satellite encounters with altitudes from 20,000 to 80,000 km. The nontargeted satellites are denoted in Table 1 with an A following the encounter number. (These nontargeted satellites did not contribute significantly to trajectory shaping.) A solar conjunction occurred during Galileo's fifth orbit of Jupiter, and so there is no targeted encounter associated with orbit 5. A trajectory pole view of Galileo's first 12 orbits around Jupiter is shown in Fig. 1.

Spacecraft Tracking Systems

Galileo is tracked with two-way coherent S-Band radio transmissions via the NASA Jet Propulsion Laboratory (JPL) Deep Space Network's 70-m antennas in Goldstone (California), Canberra (Australia), and Madrid (Spain). Data consist of Doppler measurements extracted from the radio signal as well as optical images acquired with the onboard digital spacecraft camera. Optical data compliment the Doppler, providing an orthogonal component to the data set.

Our ability to determine the orbit of Galileo degraded when the high-gain antenna failed to open after launch. The extant remaining low-gain antenna operated less efficiently by a factor of 40 dB. This attenuation limited the number of optical navigation images returned to Earth, although this limitation was partly overcome by placing software onboard Galileo to compress and edit the frames before downlinking to Earth.

The optical images consisted of one (or more) Galilean satellites shuttered against a reference stellar background. The camera's field-of-view is 10 μrad per pixel with an accuracy of 0.33 pixel (1σ). Combined with ground-based astrometry, it was possible for this procedure to obtain star-relative satellite position knowledge of 15 km. This determination provided valuable information on satellite mean longitude and out-of-plane state, two parameters essentially invisible to radiometric data. Dynamical knowledge could

Table 1 Satellite encounter geometry and dates

Encounter	OWLT,[a] min	Inbound/ outbound	Date, SCET[b] ± s	Altitude, km	Latitude, deg
G1	35	In	27-June-96 06:29:06.70 ± 0.005	835.22 ± 0.03	30.39 ± 0.002
G2	39	In	06-Sept.-96 18:59:33.88 ± 0.02	260.65 ± 0.50	79.28 ± N.A.
C3	46	In	04-Nov.-96 13:34:28.00 ± 0.005	1135.96 ± 0.04	13.19 ± 0.002
E3A	46	Out	06-Nov.-96 18:49:51.31 ± 0.07	34,786.51 ± 1.45	0.70 ± 0.026
E4	50	Out	19-Dec.-96 06:52:57.70 ± 0.01	692.05 ± 0.10	−1.67 ± 0.036
E5A	51	Out	20-Jan.-97 01:08:37.00 ± 0.31	26,667.83 ± 0.29	−0.82 ± 0.007
E6	50	In	20-Feb.-97 17:06:10.20 ± 0.01	586.33 ± 0.07	−17.02 ± 0.004
E7A	46	In	04-April-97 05:58:47.56 ± 0.05	23,487.08 ± 0.31	2.14 ± 0.005
G7	46	Out	05-April-97 07:09:58.10 ± 0.005	3101.85 ± 0.04	55.80 ± < 0.0005
C8A	42	In	06-May-97 12:10:27.75 ± 0.67	33,060.56 ± 0.46	−42.00 ± 0.001
G8	42	In	07-May-97 15:56:09.55 ± 0.005	1603.24 ± 0.03	28.271 ± 0.001
C9	36	In	25-June-97 13:47:49.95 ± 0.005	418.09 ± 0.03	1.96 ± 0.012
G9A	36	In	26-June-97 17:19:34.31 ± 0.005	79,741.06 ± 0.18	−0.02 ± 0.011
C10	35	In	17-Sept.-97 00:18:54.78 ± < 0.001	535.31 ± 0.01	4.60 ± 0.004
E11	41	In	06-Nov.-97 20:31:44.21 ± 0.003	2043.26 ± 0.03	25.73 ± 0.001
G12A	47	In	15-Dec.-97 09:58:09.34 ± 0.002	14,402.54 ± 0.03	−5.82 ± 0.001
E12	47	Out	16-Dec.-97 12:03:19.86 ± 0.001	200.99 ± 0.15	−8.68 ± 0.003

[a]One-way light time. [b]Spacecraft event time (UTC). To compute Earth received time, add OWLT to SCET.

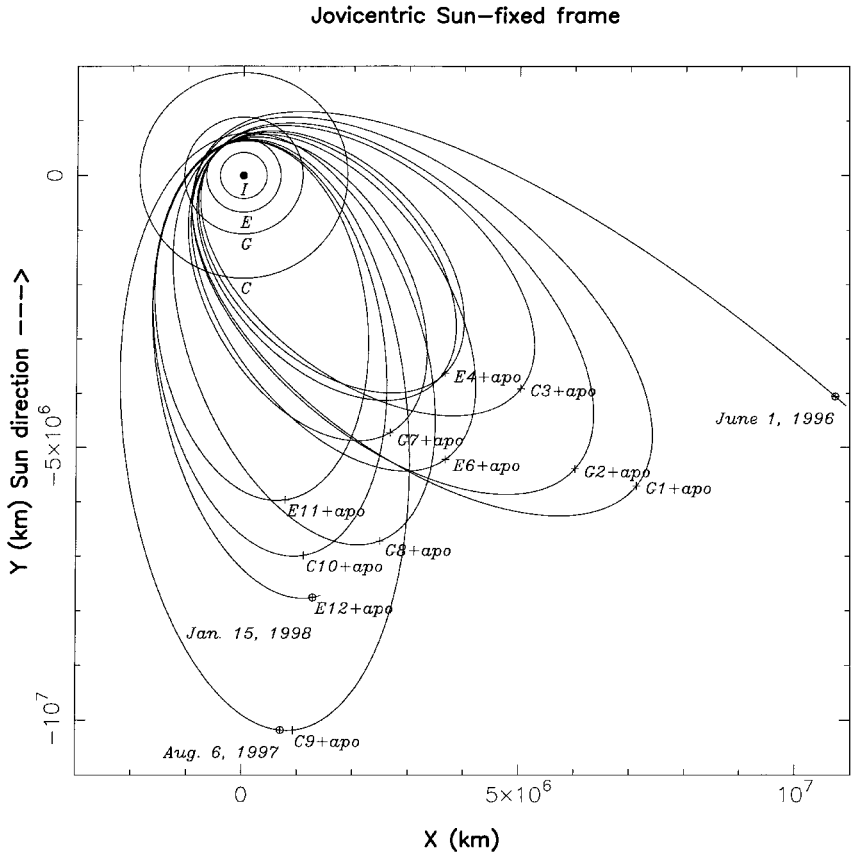

Fig. 1 Galileo satellite tour from June 1996–January 1998.

in turn be inferred for the remaining three satellites—either Io, Europa, or Ganymede (from their Laplacian resonance), and to a lesser degree, Callisto.

For the first six encounters (G1–G7), 8–33 images per orbit were returned, yielding a total of 138 for the mission. Optical images for navigation purposes were not acquired after G7.

The Doppler quality was consistent with a typical data rms of about 0.3 mm/s. Only during solar conjunction (January 1997) was a significant increase in this noise level observed (because of the passage of the radio signal through the solar corona). Except for this conjunction period, we attached an a priori data accuracy to the Doppler of 2.5 times the rms of the residuals for each tracking pass (with a lower bound of 0.5 mm/s). In practice the data weights varied between 0.5 mm/s and (rarely) 10 mm/s.

Satellite Ephemeris (Integrated vs Theory)

Prelaunch navigation studies were founded on analytical satellite ephemerides, which computationally limited satellite knowledge to ~10 km, the limiting accuracy of this ephemeris.[10] Postlaunch studies showed, however, that the analytical ephemeris was not consistent with an integrated satellite ephemeris. Large secular and periodic downtrack differences existed, and ground-based observational data of Jupiter's moons strongly supported the integrated ephemeris (private communication by R. A. Jacobson, JPL, Pasadena, California, May 1996). Therefore the Galileo project decided in favor of an integrated satellite ephemeris, and in May 1996 a baseline integrated ephemeris (and satellite covariance) was released for tour navigation (Jacobson, personal communication). For future reference we will denote this satellite ephemeris as JUP088.

Orbit Determination

To determine the orbits of the spacecraft and satellites a least-squares fit to the observations was performed. The satellite ephemerides were iteratively improved based on the least-squares solution. The procedure followed well-established techniques employing a batch sequential pseudo-epoch-stateleast-squares filter.[11] The adjustable parameters in the filter model included the epoch state of Galileo and each satellite, spacecraft thrusting events, solar radiation pressure, satellite masses and gravity fields, and Jupiter's mass, ephemeris, and orientation parameters. A detailed description of the Galileo model is discussed in Ref. 3.

We wish to make a point of the solar radiation pressure model. In general the model was stable and consistent, and we saw no evidence for unmodeled gravitational forces.[12] During the Jupiter approach phase however (before the tour), we discovered that spacecraft thermal emissions emanating from the subsolar direction (especially from the radioisotope thermal generators) were of similar magnitude to the solar radiation pressure—in effect decreasing the solar radiation pressure. This contribution was consistently determined to be 0.4 nm/s^2 (cf. solar radiation pressure determination of 3.3 nm/s^2 at 5.2 astronomical units). During the tour, to reduce the number of estimated parameters the spacecraft's thermal emission was combined into the solar pressure model (effectively lowering the reflectivity coefficients).

Orbit Trim Maneuvers

Trajectory control in orbit was provided with periodic thrusting events, or orbit trim maneuvers (OTMs). Three OTMs were planned per orbit (more if needed). Maneuvers at apojove were often designed to change the spacecraft's orbital characteristics to meet tour objectives (such as steering for an Io occultation). Preencounter and postencounter OTMs were designed to remove navigation errors, nudging the spacecraft back to the correct path. These maneuvers occurred approximately three days before and three days after each satellite encounter. The preencounter maneuver was often modified one week after the original design (but still before the encounter) with recent tracking data. The new data usually led to an updated maneuver design, as a "tweak," which reproduced the intended trajectory more accurately than the initial design. After the satellite flyby the future path was reoptimized by adjusting trajectory targets at the remaining satellite encounters (using propellant consumption as the cost function). Reoptimization was constrained to only allow changes in subsequent targets by ±50 km in latitude and cross latitude (altitude) and by ±3 min.

Navigation Results

An insertion burn placed Galileo into orbit around Jupiter on 8 December 1995.[7] Between that time and 1 June 1996 four additional maneuvers occurred, including a maneuver on 14 March of magnitude 376 m/s to raise the perijove of Galileo and send the spacecraft on to Ganymede, the first encounter of the tour. The results described herein begin 1 June, 26 days before Ganymede. As an illustration of the navigation procedure, we summarize this first encounter in moderate detail. (A detailed description of the first nine encounters can be found in Ref. 3.) Following this, a tour summary of performance results and comparison with predictions for G1 through E12 is provided.

G1 Approach and Encounter

The first G1 targeting maneuver, designated OTM-5, occurred 12 June, 15 days before G1. The maneuver was designed with Doppler data spanning 8 December 1995–5 June 1996. This arc also included two distant optical navigation images of Ganymede. The residual scatter in these data were 0.006 mm/s rms for the Doppler and 0.17 pixel rms for the optical, apparently indicating a good match between the data and the model. But the solution incorporating these data determined the spacecraft to be following a trajectory that missed the target by 907 km and 131 s (Table 2). The Ganymede ephemeris uncertainties at the time of this solution were 9.7, 41.5, and 71.3 km in the **CT**, **DT**, and **OOP** directions, respectively (1σ). These uncertainties were significantly smaller than the trajectory errors. Therefore by incorporating the optical and Doppler data into the spacecraft/satellite solution, the relative spacecraft-Ganymede separation was determined, and Ganymede's position was found to be in error by -4.5 ± 9.6 km in **CT**, -32.6 ± 40.9 km in **DT**, and 5.1 ± 71.3 km in **OOP**—a substantial error, but still subsigma. The uncertainty of Ganymede in this solution did not improve substantially because the time series of two images, at that range, was insufficient to improve upon the a priori ephemeris uncertainty.

Using the updated ephemeris information, OTM-5 thrusted with a ΔV of 0.53 m/s to redirect Galileo to the G1 aimpoint. One more maneuver three days before the encounter on 24 June (OTM-6t, with the tweak DCO on 23 June) further refined the inbound trajectory. A total of 33 images were shuttered on this inbound leg with a success rate of 76%.

The first post-G1 solution, a reconstruction of the G1 encounter with a posteriori data, determined the spacecraft position at the time of the encounter to be in error by less than 1σ, missing the aim point by 0.5σ in both $\boldsymbol{B}\cdot\boldsymbol{R}$ and $\boldsymbol{B}\cdot\boldsymbol{T}$ (-8.8 km, -15.3 km) and 1.6σ in $\boldsymbol{B}\cdot\boldsymbol{S}$ (late by 2.7 s). The postencounter determination of Ganymede's ephemeris showed a shift of -16 km (2σ) in **CT**, -22 km (0.7σ) in **DT**, and -6 km (0.4σ) in **OOP** with respect to JUP088.

A postencounter maneuver (OTM-7) was implemented to correct the encounter errors. To apply the ephemeris knowledge acquired at G1 to future encounters, the JUP088 ephemeris and covariance were updated and incorporated into post-G1 solutions. The post-G1 orbit solution for the design of OTM-7 determined that the second orbit's period was short of the design value by approximately 63 min. OTM-7 corrected this energy error, thrusting on 30 June 1996 with a ΔV of 0.59 m/s ± 0.01%. Afterward the G2 aimpoint was selected, thereby fixing the flyby of Ganymede-2 at an altitude of 262 km on 6 September 1996 18:59.0 UTC.

An apojove maneuver to adjust the inclination of the spacecraft's orbit was also required in order to reach G2. The apojove maneuver, OTM-8, occurred on 5 August 1996 with a ΔV of 4.60 m/s ± 0.14%. A G2 preencounter maneuver (three days before G2) was planned to further refine the inbound trajectory, but calculations performed at that time determined that the spacecraft orbit uncertainties were dominated by the Ganymede ephemeris uncertainty. The preencounter maneuver therefore was cancelled.

Table 3 summarizes navigation performance during the prime mission (plus E12) and compares these results with the predicted errors from earlier studies. The results are quantified in terms of B-plane parameters (except for altitude). Note that as the tour progressed, the magnitude of the miss vector $|\Delta\boldsymbol{B}|$ decreased. This improvement was a direct consequence of increased satellite ephemeris knowledge. We also note that for all encounters except Ganymede-2 the actual errors were less than or approximately equivalent to the predicted errors. (The relatively large errors at Ganymede-2 vis-a-vis predictions resulted from a Galileo project decision to cancel the preencounter maneuver.) By the time of Europa-12, the dynamics of the Jovian system were known well enough to place the spacecraft within 1 km of its Europa target.

Table 2 Ganymede-1 B-plane (encounter on 27 June 1996 6:29:07 UTC)

Date	OTM	DCO[a]	$\boldsymbol{B}\cdot\boldsymbol{R}$, km	$\boldsymbol{B}\cdot\boldsymbol{T}$, km	TCA,[b] SCET UTC	σSMA,[c] km	σSMI,[d] km	Θ, deg
Target	——	——	−1835.7	3157.9	06:29:04.0			
June 5	5	G1−22d	−1717.0 ± 73.2	4056.9 ± 48.0	06:26:53.3 ± 5.14	73.3	47.8	86.0
June 16	6	G1−11d	−1837.9 ± 23.4	3189.3 ± 40.9	06:29:00.5 ± 4.03	41.0	23.3	175.7
June 23	6t	G1−3.5d	−1860.4 ± 16.2	3236.4 ± 30.5	06:28:55.0 ± 1.65	30.7	15.9	172.9
June 27	7	G1+10h	−1844.4 ± 0.1	3142.9 ± 0.1	06:29:06.7 ± <0.05	0.1	<0.05	53.3
July 26	8	G1+apo	−1844.5 ± 0.3	3142.6 ± 0.2	06:29:06.7 ± <0.05	0.4	0.1	66.0

[a]Data cutoff. [b]Time of closest approach. [c]Semimajor axis. [d]Semiminor axis.

Table 3 Navigation performance summary

	Encounter delivery error relative to target					1σ predicted error[5,6]			
Encounter	$\Delta \boldsymbol{B} \cdot \boldsymbol{R}$, km	$\Delta \boldsymbol{B} \cdot \boldsymbol{T}$, km	$\lvert\Delta \boldsymbol{B}\rvert$, km	Δaltitude, km	ΔTCA, s	$\Delta \boldsymbol{B} \cdot \boldsymbol{R}$, km	$\Delta \boldsymbol{B} \cdot \boldsymbol{T}$, km	$\lvert\Delta \boldsymbol{B}\rvert$, km	ΔTCA, s
Ganymede 1	−8.8	−15.3	17.6	−8.8	2.7	14.7	21.0	25.6	1.0
Ganymede 2	3.7	13.1	13.6	−1.2	−5.1	9.0	3.0	9.5	0.2
Callisto 3	14.0	22.1	26.2	18.2	0.7	19.0	42.0	46.1	1.6
Europa 4	11.2	6.3	12.8	−6.1	1.1	10.0	5.0	11.2	1.6
Orbit 5	Solar conjunction, no targeted encounter								
Europa 6	9.6	2.3	9.8	0.4	−2.8	13.0	3.0	13.3	0.7
Ganymede 7	−2.1	−9.8	10.0	7.3	−0.2	20.0	16.0	25.6	0.6
Ganymede 8	−0.4	−8.4	8.4	7.5	0.2	10.0	17.0	19.7	0.2
Callisto 9	1.0	−3.0	3.2	3.0	0.1	7.0	8.0	10.6	0.8
Callisto 10	−4.7	−3.4	5.8	−2.9	−0.2	11.0	7.0	13.0	0.4
Europa 11	−19.1	−8.0	20.7	0.8	0.8	20.0	8.0	21.5	2.5
Europa 12	0.5	0.9	1.0	1.0	−0.1	4.5[a]	9.4[a]	10.5[a]	1.2[a]

[a]Computed in April 1997.

Table 4 Satellite ephemeris differences between subsequent encounters

Encounter	Satellite	Δ**CT**, km	Δ**DT**, km	Δ**OOP**, km	Data arcs (begin, end)
G1	Ganymede	−16.99	−39.25	−1.98	G1−1month − G1+apo
G2	Ganymede	0.20	−8.13	6.57	G1+apo − G2+apo
C3	Callisto	−2.04	−23.84	15.41	G2+apo − C3+apo
E4	Europa	−1.40	16.08	17.38	C3+apo − E5A+apo
E6	Europa	−0.17	7.54	−0.98	E5A+apo − E6+apo
G7	Ganymede	−0.13	−3.91	3.73	E6+apo − G7+apo
G8	Ganymede	−0.03	0.40	0.21	G7+apo − G8+apo
C9	Callisto	−0.41	1.49	−0.12	G8+apo − PostC9
C10	Callisto	−0.07	0.20	−1.57	PostC9 − PostC10
E11	Europa	6.31	6.64	20.4	PostC10 − PostE11
E12	Europa	−0.02	−0.32	−2.13	PostE11 − PostE12

Table 5 Satellite position differences from JUP088 for the epoch 1 January 1998

Satellite	Δ position at epoch, km, rss	1σ position uncertainty as of 1 Jan. 1998, km, rss	1σ position uncertainty as of Nov. 1995 (JUP088), km, rss
Io	7	±4.9	±42
Europa	54	±0.6	±80
Ganymede	28	±0.9	±78
Callisto	55	±3.8	±50

Satellite Ephemeris Improvement

The Galilean satellite positions were known to approximately 50 km root sum square (rss) (1σ) at the time of Galileo's arrival.[7] With on-orbit data knowledge, the satellite ephemerides improved by two to three orders of magnitude at encounter times and approximately one order of magnitude elsewhere (i.e., to better than 5 km as of 1 January 1998). This continuous improvement of satellite ephemerides as the tour progressed contributed to the successful navigation of Galileo.

Table 4 illustrates the incremental position change occurring between subsequent encounters. Relatively large movements took place early in the tour, after the first and/or second encounter with each respective satellite. One exception to this pattern was E11, where a change of 22 km rss occured close to the end of the nominal tour. Uncertainty in Europa's node caused that out-of-plane shift, occasioned by a dearth of recent Europa encounter data. To contrast, Ganymede and Callisto ephemerides remained up to date because of occasional nontargeted flybys interspersed throughout the tour (see Table 1). For E11 because optical information was not acquired, the last direct position information of Europa was nine months earlier at E6.

We present another metric of ephemeris improvement in Table 5. Table 5 compares JUP088 with an ephemeris computed after the E12 encounter, i.e., JUP088 is compared with a later revision of itself incorporating data from all 11 encounters. These satellite ephemerides are compared for the epoch 1 January 1998. The table also shows the corresponding improvement in our assessment of the accuracy of that epoch state (i.e., the ephemeris uncertainty). The adjustments are all subsigma with respect to JUP088.

Jupiter Ephemeris Improvement

The Jupiter ephemeris we computed in June 1996 (shortly before the first Ganymede encounter) was observed to have shifted −177 km in **OOP** and 8 km in **DT** with respect to the Jupiter-arrival ephemeris computed six months earlier (a 3σ-shift in **OOP**).[7] The earlier ephemeris was not sufficiently sensitive to Jupiter's out-of-plane component (minimal data acquired after the Jupiter encounter and possibly significant mismodeling of the Jupiter orbit insertion burn) although that arrival ephemeris had also shifted significantly with respect to the baseline ephemeris DE-143. The June solution, buoyed by an additional six months of postencounter data, continued the out-of-plane correction. (The out-of-plane problem was well known at the time of Jupiter arrival, but an ephemeris solution was required at that time for probe reconstruction.[7])

Our Jupiter solutions have varied over a 2σ-range since G1, as shown in Table 6. The out-of-plane component has varied most, resisting precise, consistent determinations.[13] Consequently our current operational data set provides little insight into the Jupiter out-of-plane component, although we have improved the **OOP** formal sigma by a factor of three. A rigorous solution for Jupiter's ephemeris must await a coordinate transformation to J2000 and additional analyses with more comprehensive data (i.e., inclusive of all spacecraft encounters with Jupiter).

Gravity Estimates of the Jovian System

Figure 2 illustrates changes in the Galilean satellite masses (GM) from the JUP088 a priori values vs time (27 June 1996–27 December 1997). Also shown in Fig. 2 are changes in Jupiter's mass (divided by 100) from the a priori.[14] These mass histories changed erratically through 1996, and then settled down once each of the major satellites was visited with a low-altitude encounter. Io (indicated with the solid line and + marks), the most egregious example of mass stability, was visited once but under suboptimal conditions.[7] Io encounters planned in 1999 will further improve Io's mass determination.[4]

Table 6 Jupiter ephemeris differences on 7 December 1995 w.r.t. the JPL ephemeris DE-143[a]

Date	Orbit	Δ**CT**, km	Δ**DT**, km	Δ**OOP**, km	Δd**CT**, mm/s	Δd**DT**, mm/s	Δd**OOP**, mm/s
5 Jan. 1996	JOI[b]	19 ± 2	−69 ± 5	549 ± 59	1.15	−0.18	−1.18
26 June	G1	18 ± 2	−77 ± 10	372.06 ± 76	1.25	−0.19	−5.31
6 Sept.	G2	18 ± 2	−78 ± 5	458 ± 58	1.25	−0.20	−6.40
23 Oct.	C3	18 ± 2	−71 ± 10	371 ± 59	1.12	−0.20	−5.14
27 Nov.[c]	G2-C3	16 ± 4	−76 ± 9	259.58 ± 57	1.20	−0.17	−3.86
3 April 1997	G7	14 ± 4	−71 ± 5	305 ± 38	1.15	−0.14	−4.46
10 Sept.	C10	19 ± 4	−96 ± 6	238.46 ± 22	1.42	−0.21	−5.44

[a]Heliocentric Earth mean equator (EME) 1950, Jupiter-orbit fixed, at the time of the G1 encounter.
[b]Jupiter orbit insertion.
[c]Includes two east-west and two north-south spacecraft interferometric measurements.

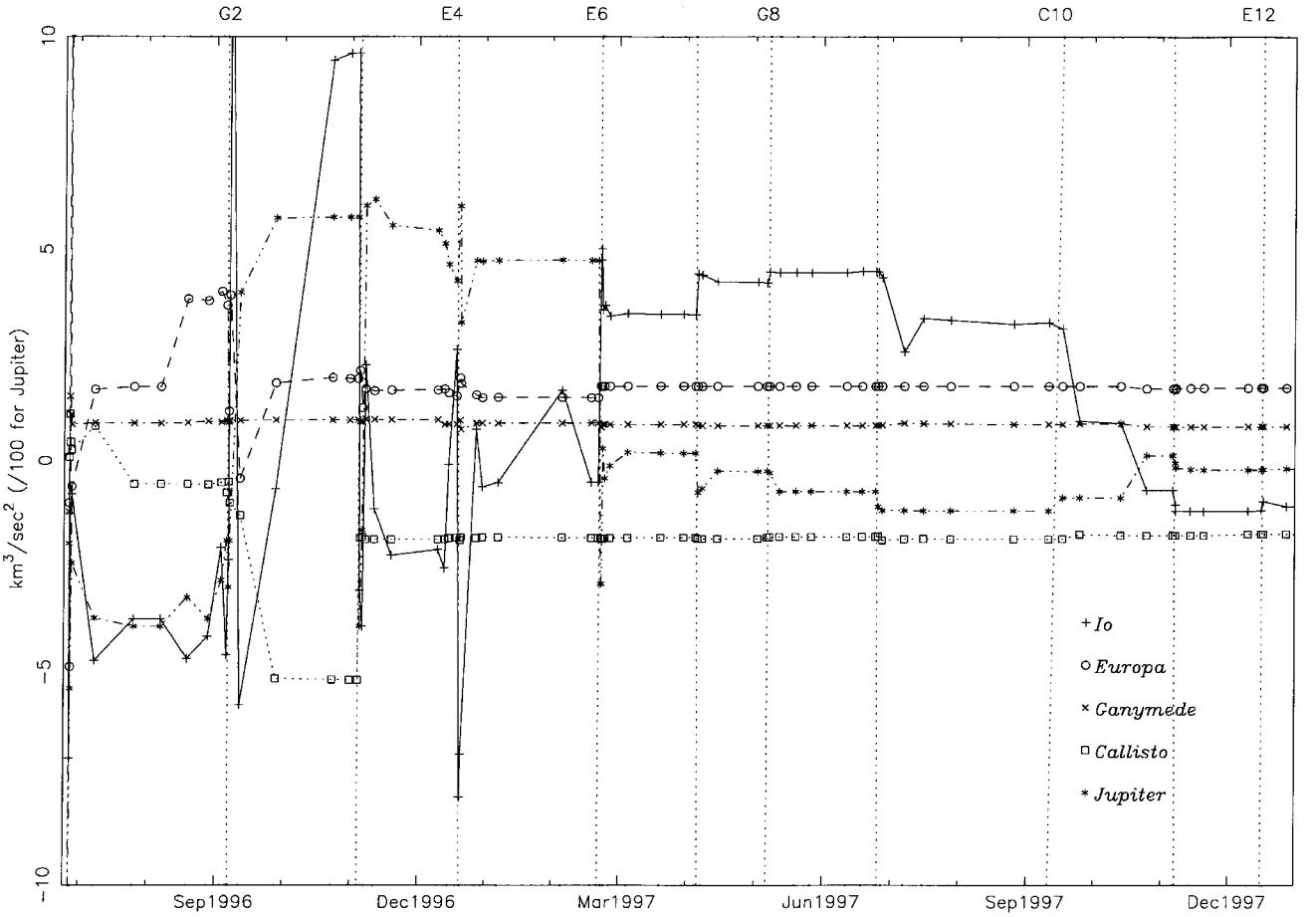

Fig. 2 Changes in Jupiter and satellite masses from a priori.

The 1σ uncertainties for the mass estimates in Fig. 2 are shown in Fig. 3. This figure indicates the improvement in mass knowledge at each flyby (i.e., the uncertainties decrease). This is particularly evident for targeted satellites. Even so, the improvement in Europa's mass after the C3 encounter can be attributed to the E3A nontargeted flyby (see Table 1). The improvement of Io's mass after C10 can also be attributed to a close passage of Io (but at a distance greater than 100,000 km and so this encounter is not noted in Table 1). The satellite ephemeris covariance was scaled by three during solar conjunction (January 1997), and so Fig. 3 shows an increase in all mass uncertainties at that time. The mass estimates for Ganymede, Europa, Callisto, and Jupiter have all been consistent since the C3 encounter.

Table 7 lists the mass, oblateness, and orientation of Jupiter. Jupiter's low-order oblateness coefficients (J_2, J_4) have not improved significantly from the a priori; all other terms in Table 7 have improved significantly from the a priori.[14] Our current estimate for Jupiter's mass has increased by 0.5σ with respect to our determination in 1996; the precision of the mass estimate has improved by a factor of 34 (Ref. 7). Figure 2 shows that Jupiter's mass estimate has undergone roughly three levels of change: between G1 and G2 (~ -40 km^3/s^2), between G2 and E4 ($\sim +50$ km^3/s^2), and after E6 (~ -10 km^3/s^2). We have not investigated whether ephemeris updates or scaling could have influenced these groupings.

Gravitational fields of the satellites (and Jupiter) have been determined; the fields are represented by spherical harmonic expansions of the gravitational potential. The field for Io has been least well determined because only a single encounter with Io has occurred as of the time of this writing (on 7 December 1995, one day before Jupiter orbit insertion, at an altitude of 897 km).[7] Thus we chose to estimate only a second order and degree field for Io. For the remaining three Galilean satellites more (and closer) encounters have occurred, and so we elected to estimate complete third degree and order fields for Europa, Ganymede, and Callisto. (But we do not report the degree three, order three, or cross terms of any degree/order because their values were not significant.) For the a priori conditions we assumed that each satellite was of uniform density and in hydrostatic equilibrium.[15] Because the coefficient J_2 could not

be determined independently of each satellite's GM and C_{22}, the hydrostatic constraint set J_2 equal to $\frac{10}{3}$ of C_{22}. The satellite gravity fields we obtained are presented in Table 8.

Analysis of these gravity fields indicates that Ganymede and Europa have differentiated into predominantly three layers: an outer water-ice shell approximately 100 km thick, a mantle of rocky material, and possibly an iron core.[15] Parts (or most) of Europa's outer shell may be liquid water, with just a thin water-ice lithosphere. High-resolution images of Europa supply indirect corroborating evidence of a global ocean. These images show a terrain nearly crater free and of low relief, with a surface apparently undergoing constant reworking. Moreover, sufficient heat to maintain a global liquid ocean on Europa can be supplied by tidal dissipation. Tidal heating can originate from the torques acting on satellites in eccentric orbits (for Europa, $e = 0.009$), thereby flexing the satellites and causing rotation to be nonsynchronous.[16] Callisto has not differentiated as completely as Europa and Ganymede and appears to consist of only two layers (water-ice and rock, mostly the former). Moreover Callisto has one of the most densely cratered surfaces in the solar system, indicating an inert body. Io appears to be similar to Europa and Ganymede in form but without the outer water-ice shell.[17] The satellite body axes also appear to be misaligned with their principal axes of inertia, where the misalignment grows progressively worse from Callisto to Io (see the S_{22} coefficient).

Table 7 Jupiter mass (km^3/s^2), gravity harmonics, and pole orientation

Parameter	Estimate
Gravity	
GM	126,712,764.99± 2.51
J_2 ($\times 10^{-6}$)	14,737.05± 0.96
J_4 ($\times 10^{-6}$)	−587.80± 5.00
Pole (EME-50)	
Right ascension, deg	268.0007± 0.0006
Declination, deg	64.5053± 0.0003

Conclusions

The comparison of navigation performance with prediction has been provided in Table 3. Except for the second Ganymede encounter (with the canceled preencounter maneuver), the predicted errors were conservative vis-a-vis the achieved results. We attribute this to our observation that the actual uncertainty during maneuver execution was appreciably smaller than the error predicted by the propulsion system designers. Additional contributing factors include: 1) our successful acquisition of Doppler data within 1 h of encounters (this had not previously been assumed) and 2) our successful application of satellite covariances derived from previous encounters (also not previously assumed). Satellite ephemeris errors tended to dominate orbit uncertainty, and so the technique of applying updated ephemerides and covariances to the current data arc brought about significant improvement to each subsequent

Table 8 Satellite masses (km^3/s^2) and gravity harmonic coefficients

Parameter	Io	Europa	Ganymede	Callisto
GM	5959.91± 0.11	3202.72± 0.01	9887.81± 0.01	7179.26± 0.02
J_2 ($\times 10^{-6}$)	1863± 423	441± 20	146± 23	25± 10
C_{22} ($\times 10^{-6}$)	547± 14	132± 1	33± 5	7± 3
S_{22} ($\times 10^{-6}$)	19± 12	9± 1	3± 5	−1± 3

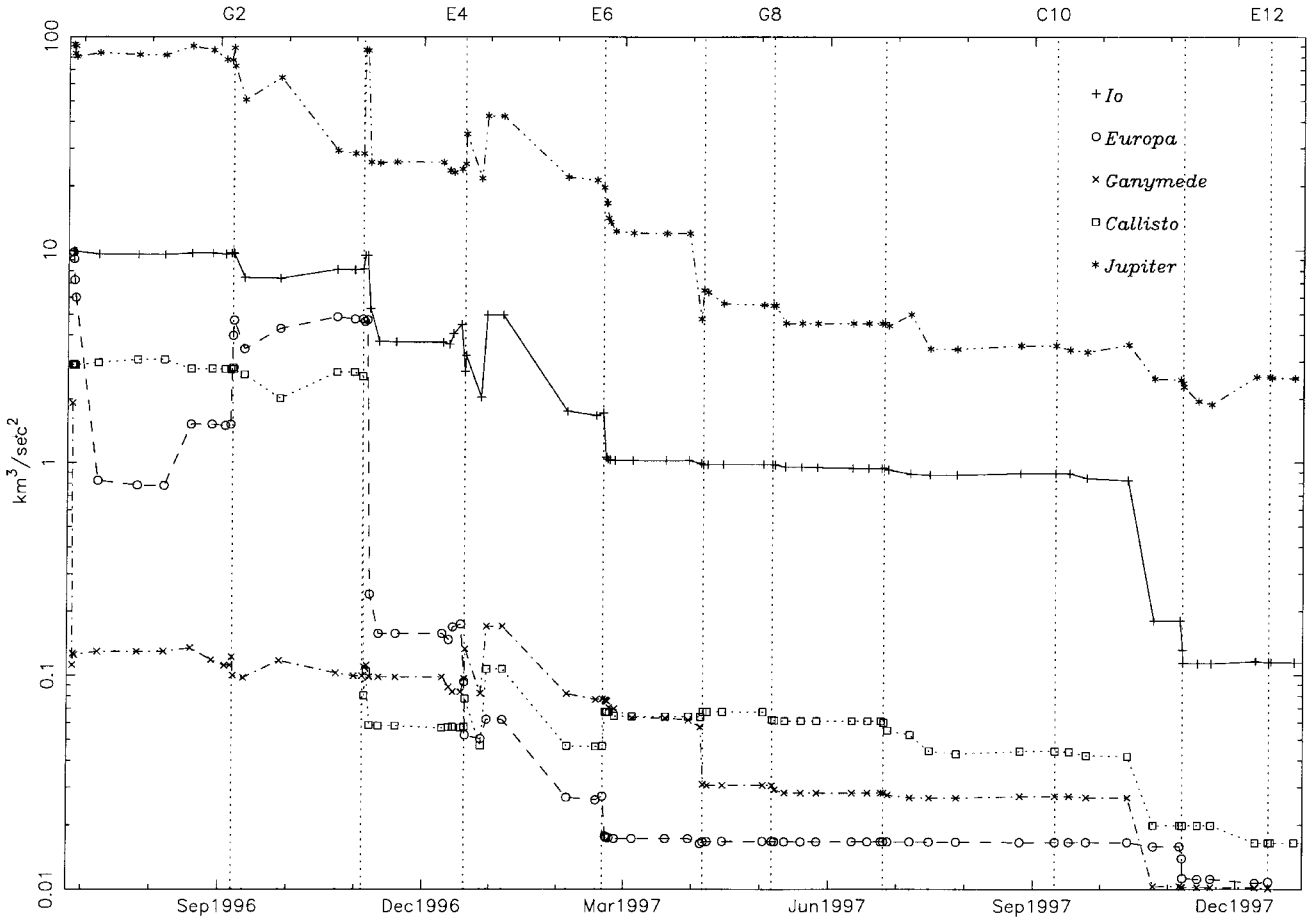

Fig. 3 Jupiter and satellite mass uncertainties (1σ).

encounter solution, as demonstrated by the convergence of the satellite ephemerides in Table 4.

By April 1997 (after six encounters) satellite locations had been determined to better than 10 km (1σ). With this ephemeris accuracy the remainder of the mission could operate without optical navigation because optical data would no longer contribute to ephemeris improvement.

The optical campaign (revised to accomodate the capability of the low-gain antenna) finished with a 64% success rate. Many optical navigation images classified as unsuccessful were the result of low-tolerance viewing opportunities created by the preencounter attitude of the spacecraft (the sunshade of Galileo obscured the target) and were not caused by systematic flaws in the design or equipment.

In addition to ephemeris improvement, knowledge of satellite masses have been improved. Gravitational parameters are now known to better than 0.2 km^3/s^2 for Io and 0.05 km^3/s^2 for Europa, Ganymede, and Callisto—factors of 50, 200, 60, and 60 respectively better than the masses determined from the Voyager and Pioneer missions. The mass estimate of Io has improved by a factor of 27 from the value obtained by several of us in 1995 at the time of the first Io encounter. Gravity fields for each of the major moons have been determined for the first time and are listed in Table 8 (the gravity field for Io has not changed from Ref. 7).

The gravity of Jupiter has been determined to better than 3 km^3/s^2, which is a factor of 30 better than the previous error bar determined at the time of Galileo's arrival at Jupiter. Errors in the B1950 pole of Jupiter have improved by better than a factor of 10 from the Voyager results.

Large shifts in Jupiter's ephemeris on the order of 70 km downtrack and 300 km out of plane ($>1\sigma$) have been observed with respect to the JPL planetary ephemeris DE-143. The Galileo project decided in 1978 to use the B1950 system so that inconsistencies between this coordinate frame and the standard J2000 frame may exist. Further analysis is needed to reconcile these discrepancies.

For the dozen orbits we have reported here, the average trajectory errors in delivering Galileo to its targeted aimpoints were 0.9σ in $\boldsymbol{B}\cdot\boldsymbol{R}$, 0.6σ in $\boldsymbol{B}\cdot\boldsymbol{T}$, and 1.6σ in encounter time (with respect to the preencounter solution). Subsigma deviations from the target resulted at the E4, E6, G7, and G8 encounters. The E11 encounter experienced the largest relative position error (3.4σ in $\boldsymbol{B}\cdot\boldsymbol{R}$), but the timing of that encounter was accurate with the moment of closest approach in error by only 0.3σ. The large position error at E11 was caused by a shortage of tracking data, the result of a project decision to begin the maneuver design procedure six days (12% of the orbit) earlier than the standard template used for all previous encounters.

The total propellant expended to navigate the 11 satellite tour (the prime mission plus E12, i.e., from 1 June 1996 to the E12 encounter on 16 December 1997) was equivalent to a ΔV of 70.2 m/s (includes the propellant necessary for path correction, maneuver implementation, and attitude maintenance). The deterministic portion of this total was 34.9 m/s, which included a 14-m/s maneuver following C10 not originally part of the nominal tour, but which was later inserted to extend the tour beyond E12 (Ref. 4). Compare the total to a ΔV of $\sim$100 m/s originally estimated for the prime mission (excluding the E11-E12 orbit, which was not part of the original design).[6]

Accurate propagations of the trajectory were achieved by continuously updating satellite ephemerides and mean motion parameters and from a laudable performance of the propulsion system. The mean maneuver magnitude underperformed by 0.3% (the expected 1σ uncertainty was $\pm 1\%$) and the mean pointing error was 65% of the a priori uncertainty of 0.28 deg (1σ). This performance resulted in the cancellation of 6 of 11 preencounter maneuvers. The resulting propellant savings was significant and may lead to as much as a four-year extension of the Galileo mission.

Appendix: Target Body Coordinate System

Hyperbolic approach trajectories are typically described in aiming plane coordinates, often referred to as B-plane coordinates (Fig. A1). The coordinate system is defined by three orthogonal unit vectors $\boldsymbol{S}$, $\boldsymbol{T}$, and $\boldsymbol{R}$, with the system origin taken to be the center of the target body. The $\boldsymbol{S}$ vector is parallel to the spacecraft hyperbolic approach velocity vector relative to the target body, whereas $\boldsymbol{T}$ is orthogonal to $\boldsymbol{S}$ and lies in the ecliptic plane (the mean plane of the Earth's orbit). Finally, $\boldsymbol{R}$ completes an orthogonal triad with $\boldsymbol{S}$ and $\boldsymbol{T}$.

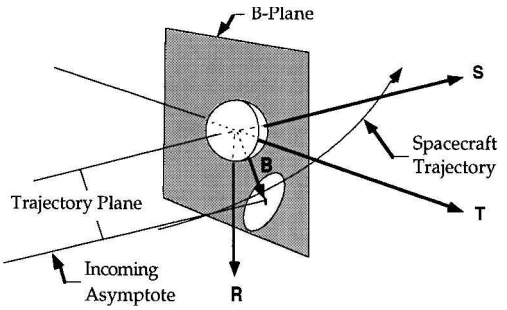

Fig. A1 B-plane coordinate system.

The aim point for an encounter is defined by the miss vector $\boldsymbol{B}$, which lies in the $\boldsymbol{T}$-$\boldsymbol{R}$ plane and specifies where the point of closest approach would be if the target body had zero mass and did not deflect the flight path. The angle θ is the rotation of $\boldsymbol{B}$ from $\boldsymbol{T}$ in a right-handed sense. The components of $\boldsymbol{B}$ along the $\boldsymbol{R}$ and $\boldsymbol{T}$ axes are referred to as $\boldsymbol{B}\cdot\boldsymbol{R}$ and $\boldsymbol{B}\cdot\boldsymbol{T}$. The time from encounter (point of closest approach) is defined by the linearized time of flight (LTOF), which specifies what the time of flight to encounter would be if the magnitude of the miss vector were zero (i.e., if the target were the origin of the B-plane). The TCA is often used interchangably with LTOF.

The uncertainty of the actual intercept point of the incoming trajectory with the B-plane prior to the spacecraft's arrival at the B-plane (caused by imperfect knowledge of the spacecraft's state, for instance) is quantified in terms of the eigenvalues of the spacecraft uncertainty covariance, mapped to the B-plane (the trajectory dispersion). The eigenvalue components of the spacecraft covariance in the B-plane are the SMA and SMI (i.e., with reference to a section through the covariance ellipsoid in the $\boldsymbol{T}$-$\boldsymbol{R}$ plane).

Acknowledgments

The work described in this paper was performed at the Jet Propulsion Laboratory, California Institute of Technology, under contract with NASA. The authors would like to express their gratitude to the following individuals for their contribution to the navigation effort: Robert Jacobson for producing the a priori satellite ephemeris and Michael Wang and Claude Hildebrand for software and optical analysis support.

References

[1]Miller, L. J., Miller, J. K., and Kirhofer, W. E., "Navigation of the Galileo Mission," AIAA Paper 83-0102, Jan. 1983.

[2]Antreasian, P. G., Nicholson, F. T., Kallemeyn, P. H., Bhaskaran, S., Haw, R. J., and Halamek, P., "Galileo Orbit Determination for the Ida Encounter," *Advances in the Astronautical Sciences 1994*, Univelt, San Diego, CA, 1994, pp. 1027–1048.

[3]Antreasian, P. G., McElrath, T. P., Haw, R. J., and Lewis, G. D., "Galileo Orbit Determination Results During the Satellite Tour," American Astronautical Society, Paper 97-699, Sun Valley, ID, Aug. 1997.

[4]Bell, J. L., and Johannesen, J. R., "Galileo Europa Mission Tour Design," American Astronautical Society, Paper 97-614, Sun Valley, ID, Aug. 1997.

[5]Haw, R. J., Kallemeyn, P. H., Nicholson, F. T., Davis, R. P., and Riedel, J. E., "Galileo Satellite Tour: Orbit Determination," American Astronautical Society, Paper 93-686, Victoria, BC, Canada, Aug. 1993.

[6]D'Amario, L. A., Brynes, D. V., Haw, R. J., Kirhofer, W. E., Nicholson, F. T., and Wilson, M. G., "Navigation Strategy for the Galileo Jupiter Encounter and Orbital Tour," *Astrodynamics 1995: Proceedings of the AAS/AIAA Astrodynamics Specialist Conference*, Univelt, San Diego, CA, 1996, pp. 1387–1411.

[7]Haw, R. J., Antreasian, P. G., McElrath, T. P., Graat, E. G., and Nicholson, F. T., "Navigating Galileo at Jupiter Arrival," *Journal of Spacecraft and Rockets*, Vol. 34, No. 4, 1997, pp. 503–508.

[8]Wilson, M. G., Potts, C. L., Mase, R. A., Halsell, C. A., and Byrnes, D. V., "Maneuver Design for Galileo Jupiter Approach and Orbital Operations," *Proceedings of the 12th International Symposium on "Spaceflight Dynamics,"* ESOC, Darmstadt, Germany, 1997, pp. 341–349.

[9]Wolf, A. A., and Byrnes, D. V., "Design of the Galileo Satellite Tour," American Astronautical Society, Paper 93-567, Victoria, BC, Canada, Aug. 1993.

[10]Murrow, D. W., and Jacobson, R. A., "Galilean Satellite Ephemeris Improvement Using the Galileo Tour Encounter Information," AIAA Paper 88-4249, Aug. 1988.

[11]Moyer, T. D., "Mathematical Formulation of the Double Precision Orbit Determination Program," Jet Propulsion Lab., California Inst. of Technology, TR32-1527, Pasadena, CA, May 1971.

[12]Seife, C., "Distant Spacecraft Seem to be Showing No Respect for the Laws of Physics," *New Scientist*, No. 12, Sept. 1998, p. 4.

[13]Hamilton, T. W., and Melbourne, W. G., "Information Content of a Single Pass of Doppler Data from a Distant Spacecraft," *Deep Space Network Space Programs Summary 37-39*, Vol. 3, Jet Propulsion Lab., Pasadena, CA, May 1966, pp. 18–23.

[14]Campbell, J. K., and Synnott, S. P., "Gravity Field of the Jovian System from Pioneer and Voyager Tracking Data," *Astronomical Journal*, Vol. 90, No. 2, 1985, pp. 364–372 .

[15]Zharkov, V. N., Leontjev, V. V., and Kozenko, A. V., "Models, Figures, and Gravitational Moments of the Galilean Satellites of Jupiter and Icy Satellites of Saturn," *Icarus*, No. 61, 1985, pp. 92–100.

[16]Peale, S. J., Cassen, P., and Reynolds, R. T., "Melting of Io by Tidal Dissipation," *Science*, No. 203, 1979, pp. 892–894.

[17]Anderson, J., Sjogren, W., and Schubert, G., "Galileo Gravity Results and the Internal Structure of Io," *Science*, No. 272, 1996, pp. 709–712.

F. H. Lutze Jr.
Associate Editor